



Changes in the physicochemical properties of isolated starch and plantain (*Musa AAB Simmonds*) flours for early maturity stage

Olga L. Torres-Vargas^{a,*}, Marcela Gaytan-Martinez^b, Castro-Campos Fernanda^b, Beatriz M. Millán-Malo^c, M.E. Rodriguez-Garcia^c

^a Universidad Del Quindío, Facultad de Ciencias Agroindustriales, Grupo de Investigación en Ciencias Agroindustriales, Quindío, Armenia, Colombia

^b Programa de Posgrado en Alimentos Del Centro de La República (PROPAC), Research and Graduate Studies in Food Science, School of Chemistry, Universidad Autónoma de Querétaro, Centro Universitario, Cerro de Las Campanas S/N, Santiago de Querétaro, Querétaro, C.P. 76010, Mexico

^c Departamento de Nanotecnología, Centro de Física Aplicada y Tecnología Avanzada, Universidad Nacional Autónoma de México, Campus Juriquilla, Querétaro, Qro, C. P 76230, Mexico

ARTICLE INFO

Keywords:

Plantain
Maturity stage
Starch
Physicochemical properties
Resistant starch

ABSTRACT

This work focuses on the study of the physicochemical changes that take place during the first stage of ripening of plantain, with particular attention to the changes in the orthorhombic and hexagonal nanocrystals present in this starch, and its relation shift with resistance starch. Significant changes were observed in the proximal analysis of plantain flour. A gradual increase in moisture content was attributed to the high content of crystalline structures and molecules that can be removed by drying. Water activity increased with ripening, which was attributed to the hygroscopic nature of the flours. The protein content increased, and the carbohydrate content decreased, indicating the progress of biochemical reactions. The changes in the fat content are consistent with the hydrolysis and resynthesis of lipids during the ripening process. The obtained results indicate a significant influence of the ripening stage on the physicochemical properties of flour and starch of plantain, which is associated with the occurrence of a climacteric peak on the 4th day of ripening.

The hydration properties of plantain flour decreased significantly during the ripening days, consistent with the occurrence of a climacteric peak. Water holding capacity (WHC) and water binding capacity (WBC) were affected by the degree of digestion of native starch granules and protein denaturation during fruit ripening. Scanning electron microscopes (SEM) showed that during ripening the surface of the isolated starches do not suffer any significant damage. X-ray diffraction patterns were used to identify crystalline structures and to study the changes in the crystalline structures. These results showed that the starch contains orthorhombic and hexagonal nanocrystals, which play an important role and which show small structural damage during ripening reflected in a decrease in their relative crystallinity. This is the first time that these nanocrystals have been studied and considered in the ripening process. Differential scanning calorimetry was used to study the thermal transition in isolated starch. The results indicated that the gelatinization of starch corresponds to the solvation of orthorhombic and hexagonal nanocrystals, and that during ripening there is a decrease in the enthalpy reflecting some crystal structural damage. Pasting properties were studied using a Starch cell for flours and isolated starches, indicating that the pasting profile is governed by intrinsic and extrinsic factors. The resistant starch does not show significant changes at this stage of maturation. This starch is the

* Corresponding author. Grupo de Investigación en Ciencias Agroindustriales, Colombia.
E-mail address: oltorres@uniquindio.edu.co (O.L. Torres-Vargas).

<https://doi.org/10.1016/j.heliyon.2023.e18939>

Received 20 May 2023; Received in revised form 31 July 2023; Accepted 3 August 2023

Available online 7 August 2023

2405-8440/© 2023 Published by Elsevier Ltd. This is an open access article under the CC BY-NC-ND license (<http://creativecommons.org/licenses/by-nc-nd/4.0/>).

one with the highest resistant starch content reported in the literature (38%). It was hypothesized that the resistant starch is directly related to the amount of whole starch granules, and more importantly, directly related to the number concentration of orthorhombic and hexagonal nanocrystals. Therefore, knowledge of the physicochemical and nutritional properties of plantain and flour at each stage of ripening allows better selection according to industrial applications.

1. Introduction

Plantain is native to Southeast Asia and belongs to the genus *Musa* in the family Musaceae. It is distributed worldwide, especially in the equatorial region which meets the requirements of sun and moisture and promotes its development. In several countries such as Colombia, Panama, Ecuador, Mexico, Costa Rica, and others, plantain is part of the human and animal diet. In some countries plantain is consumed both unripe and ripe in soups, french fries, cakes, and purees [1]. The plantain is considered one of the most important fruits in the diet due to its year-round production and flavor. In the first stages of maturity, it can be processed as flour or isolated starch for human consumption [2].

Ripening is a genetically programmed, coordinated, and irreversible phenomenon that leads to the desirable characteristics of the edible fruits. Plantain is ripe when the fruit reached a size that allows it to be separated from the plant, which is called climacteric fruit. At this stage, the fruit is considered immature. During climacteric, many biochemical reactions take place in banana, such as synthesis of ethylene, degradation of starch, accumulation of sugars, and modification of bioactive compounds [3].

The most relevant advantages for plantain flour have been, the composition of micro and macronutrients, as phenolic and flavonoid contents, and specially its high content of total resistant, and its low glycemic index thus it can be a functional food [4,5].

Several studies reported resistant starch content without considering the ripeness of the banana resulting in a wide variation in the reported values. It has been reported values for total starch content of (73.4%) and resistant starch (17.5%) [6], resistant starch content in green banana flour between 30 and 57% [7] resistant starch content in commercial green banana flour (4–62%) which was due to the different maturity stages [8], and for green banana flour 76.77% total starch and 48.99% resistant starch.

In humans, digestible starch is susceptible to hydrolysis by salivary and pancreatic α -amylases, which hydrolyze α -1 4-glycosidic bonds. Starch that reaches the colon without being fully digested is called resistant starch (RS) [9].

Resistant starch is the indigestible starch that passes through the small intestine into the large intestine where it is fermented [10–12]. The undigested starch enters the distal small intestine and hindgut for microbial fermentation. These fermentative metabolites have a positive effect on the maintenance of intestinal integrity and thus immunity, as well as on modulating, and modulation of the microbial community in part by suppressing the growth of pathogenic bacteria while selectively promoting beneficial microbes [10].

As a result of digestion, 1 g of starch provides the organism with an amount of energy equivalent to about 4 kcal (16.7 kJ). However, it has been observed that certain portions of starch may be incompletely digested after consumption and remain intact or partially hydrolyzed to pass through the small and large intestines. The term “resistant starch” (RS) was developed to describe this particular type of starch. Resistant starch can also be described as the difference between the amount of starch exposed to the action of amylolytic enzymes and the amount of starch converted to glucose during its hydrolysis [12]. Resistant starch (RS) is the fraction of starch that can resist enzymatic hydrolysis and enter the colon, where it is fermented by the intestinal microbiota. However, it is not known which components of starch reach the intestine.

It is believed that regular consumption of plantain and plantain flour has a beneficial effect on human health. In plantain, the ratio of resistant starch/total starch is more than 60% [13]. However, the content of resistant starch decreases dramatically during the ripening process banana fruit, because the resistant starch content is affected by different plantain cultivars and maturity, due to the differences in the microstructure and physicochemical properties of starch granules within plantain starch samples at different stages of maturity [14].

One of the problems related to the interpretation of the different physicochemical properties of starch is their definition. Recently, starch was defined as micron or submicron sized particles based on morphology studies. Physically, it is formed by amorphous and crystalline structures. Chemically, it is composed of free and bound water, fat, proteins, sugars, minerals, ions, and amorphous amylose and amylopectin macromolecules. Each of these elements plays an essential role in its physicochemical properties. But they introduce the orthorhombic and hexagonal nanocrystals as part of the starch components [15].

Regarding the structural characterization of the crystalline structures in isolated plantain starch, it was showed that the starch consists of orthorhombic (A-type) and hexagonal (B-type) structures indexed by Ref. [16]. These results show that this starch can be classified as C-type. This fact does not mean that the C-type is a new crystalline structure but should be understood as the simultaneous presence of both crystalline structures. However, the information on the changes of crystalline structures as a function of maturity is scarce.

In view of the work analyzed above, the aim of this study was to investigate the changes in physicochemical properties of different components of isolated starch and plantain flour at an early stage of maturity. But with special focus on the structural changes that suffer nanocrystals present on it, and finally to determine the component of this starch that contributes with the resistance starch.

2. Materials and methods

2.1. Plantain

Dominico Harton plantains (*Musa AAB Simmonds*) harvested after eight weeks of flowering in Calarcá, department of Quindío, Colombia, at an altitude of 1551 masl, an average temperature of 22.5 °C, and 76% relative humidity. Plantains at maturing stage 1 (entirely green) was selected for the study due to the highest content of starch compared to the other maturing stages. The plantains were harvested approximately 100 days after anthesis and were not exposed to any maturation treatments [17].

To prepare flour, after peeling, they were cut in slices 3 mm thick and submerged in cool water (4 °C) for 1 h to avoid oxidation, fermentation, and the use of potassium metasilfide solution. The slices were dried in a furnace at 40 °C, for 8 h. The fruits were divided into three stages, according to their stages of maturing, considering the color of the skin, that is, 1 = green; 2 = green with yellow strokes; 3 = more green than yellow. Fig. 1 a–e shows the changes in the ripening as a function of the time. The day 1 and 2 the plantains presented a color 1: green (Fig. 1 a and b), on days 3 and day 4 the plantains presented a color 2 (Fig. 1 c and d): green with yellow strokes and on day 5: the plantains presented one color 3: more green than yellow (Fig. 1 e).

2.2. Isolated starch

The isolation of plantain starch was performed by using the method proposed by Ref. [1]. The central half of the immature plantains was removed before they were peeled and sliced. Using a Kurp mixer for 3 min at 4 °C, 200 g of the sample was macerated with 400 g of cool distilled water. The slurry was centrifuged at 2800 rpm for 20 min after being held at 4 °C till precipitation. Three times, distilled water was used to wash the sample. The starch was then dried in an oven at 40 °C for 8 h.

2.3. Physicochemical properties of the plantain flour

The pH values were determined using a pH meter (HANNA Instruments, Woonsocket, USA). According to approved Method 44–19 (AACC, 2000) [18]. Readings were taken on three replicate samples and averaged. A hand-held refractometer (ATAGO N1, California, USA). The water activity (a_w) is a measure of the availability of water in food for microbial growth, was measured by an Aqualab device (Decagon Devices, Washington DC, USA) at 24 °C.

The moisture content of the samples was reduced at 60 °C for 16 h (Method 925.40; AOAC [19]) using a Sartorius MA35 moisture analyzer. The lipid content was determined using the Soxhlet extraction method [19]. The Kjeldahl method was used to determine samples' protein content (% N \times 6.25) Method 923.03; AOAC 2000 using DK 42/26 Digestor Kjeldahl. The ash content was determined using [20]. Carbohydrate content was obtained by difference of 100 g minus the sum of grams of moisture, fat, protein, and ash.

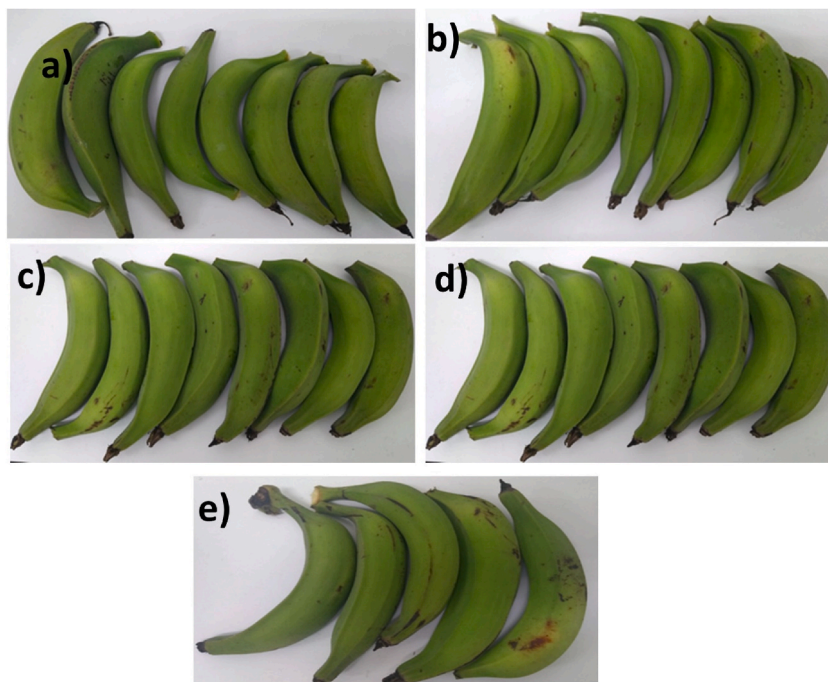


Fig. 1. a to e shows Images of plantains along maturity from day 1 to day 5.

2.4. Flour hydration properties

Water holding capacity (WHC) and water binding capacity (WBC) were determined at different day maturation of plantain to assess hydration properties of flours. These properties were determined according to the procedure described by Ref. [21]. The swelling oil absorption capacity (OAC) and the swelling volume (SV) was determined following the method reported by Ref. [22], with slight modification, using Equations (1)–(4). Emulsifying Capacity (EmC) is defined as the amount of fat that can be emulsified in a gram of sample was determined following the method reported by Ref. [21].

$$WHC \left(\frac{g}{g} \right) = \frac{\text{Weight of sediment after draining supernatant} - \text{Sample dry weight}}{\text{Sample weigh}} \quad (1)$$

$$WBC \left(\frac{g}{g} \right) = \frac{\text{Weight of sediment after centrifugation} - \text{Sample dry weight}}{\text{Sample weigh}} \quad (2)$$

$$SV \left(\frac{ml}{g} \right) = \frac{\text{Total volume of swollen sample}}{\text{Sample weight}} \quad (3)$$

$$OAC \left(\frac{g}{g} \right) = \frac{\text{Weight of sediment after draining oil} - \text{Sample weight}}{\text{Sample weigh}} \quad (4)$$

The color of plantains samples was assessed by using a Hunterlab Spectrocolorimeter (Hunter Lab Mini Scan Plus Colorimetric, USA). The color parameters were defined using the CIE L*a*b* system, where L* (L* = complete black and L* = 100 perfect white), a* (-a* = greenness and +a* = redness) and b* (-b* = blueness and +b* = yellowness) values were calculated following the method reported by Ref. [23].

2.5. Morphological analysis

Using a high vacuum scanning electron microscope (JEOL, JSM-6060LV) with a resolution in HV mode, SEM images of the separated plantain starches for various maturation stages were examined. With the help of carbon tape, each sample was secured on a specimen holder before being gold-sputtered. 20 kV electron acceleration voltage and 12–20 Pa pressure were the analysis conditions.

2.6. Structural characterization of isolated starches

On a Rigaku-Ultima IV diffractometer, isolated plantain starches were subjected to X-ray diffraction patterns analysis. The observations were made on a 2° scale from 5 to 35° while operating at 35 kV and 15 mA with a CuK_α radiation wavelength of = 0.1540 nm. To improve the intensity and resolution of each potential diffracted peak. The patterns were performed using High-Resolution X-ray diffraction with a step size of 0.01°. Samples of powder were placed into an aluminum pan. The relative crystallinity percentage was obtained using the method proposed by Ref. [18].

2.7. Differential scanning calorimetry: thermal properties

The plantain flours and isolate starches were analyzed by differential scanning calorimetry using a DSC 142 Mettler Toledo, model 821, Greifensee, Switzerland. Prior to the test, 0.5 g of the sample was placed in an airtight bag with a 60% moisture adjustment and held for 30 min 10 mg of each sample was then added and sealed in a 40-L aluminum standard pan. According to Ref. [24], the pan was heated up from 30 to 125 °C at a rate of 10 °C/min. The gelatinization endotherm and the amylose-lipid fusion endotherm enthalpy (DH) were computed from the onset (T_o), peak (T_p), and endset (T_e) temperatures.

2.8. Pasting properties

The viscosity profiles of plantain isolated starches as a function of maturity were investigated using a starch cell of an Anton Paar rheometer model MCR 102 (St Albans, United Kingdom). Each sample was heated from 50 to 92 °C for 5.3 min, and then maintained at this temperature for 5.3 min. Following this, the samples were cooled to 50 °C for 5.3 min and maintained at this temperature for 1 min 193 rpm was the consistent frequency used for all tests. The transition regimen included the pasting profiles for every investigated starch [25].

2.9. Functional groups: FT-IR analysis

The vibratory states of isolated starches were investigated using Fourier transform infrared spectroscopy. On a PerkinElmer Spectrum Two with an ATR (attenuated total reflectance) accessory and a diamond crystal, spectra were taken with a spectral resolution of 2 cm⁻¹ in the range of 600–4000 cm⁻¹.

2.10. Resistant starch

The quantification of the resistant starch content in the isolated starches and extruded starches was carried out by using the Megazyme International kit “K-RSTAR” (Wicklow, Ireland), following the certified methods of the AOAC 2002 (method 2002.02) and AACC (2001) (method 32–40.01) [18].

2.11. Design and analysis of experiments

The analyzes were carried out as independent experiments in duplicate or triplicate. Data were expressed as mean \pm standard deviation. Statistical analyses were made using Statgraphics Centurion 18 (Statistical Graphics Corporation, UK). Multiple sample comparison was used to determine significant differences among samples by analysis of variance (ANOVA) and multiple range tests. The significance level was set at P-value <0.05 , with a confidence interval of 95%.

3. Results and discussion

3.1. Physicochemical characteristics

The proximate composition of the plantain flours is shown in Table 1. The results show that the degree of ripeness has a significant effect on the chemical composition of the flour ($P < 0.05$), confirming previous results with immature and ripe banana flour [3]. The ripening days used in this study correspond to the scale proposed by Ref. [26], which is based on the number of soluble solids and gives a different color scale. Accordingly, days 1–3 (completely green) had between 1.1 and 2.0° Brix, and days 4 and 5 (green with yellow lines) had between 2.2 and 2.4° Brix. TSS increased during the plantain ripening days. The pH decreased all the time and showed lower values in the fruits with higher harvest age. The values found varied from 6.22 at harvest to 6.10 at overripening and agreed with those values found by Ref. [27] for Dominico Hartón from 6.10 to 5.09. Water activity increased with time due to the hygroscopic nature of the flours. Hygroscopicity is due to the achievement of equilibrium between the product and the environment at certain relative humidity and temperature conditions.

During the ripening days a gradual increase in the moisture content of plantain flour was observed which is due to the high content of crystalline structures and a large amount of water molecules that can be removed by drying. The maximum moisture content of plantain flour was 7.23, which is lower than the recommended value for fruit powder (13%) and is stable against microbial decay [28]. The above results could be due to ethylene production and respiration rate during ripening of plantain. Ethylene production could start on the 4th day of ripening and show strong ethylene production on the 5th day. Day marking the beginning of the climacteric phase. After the fifth day of maturation, ethylene production can rapidly decrease to a very low level [29]. During the ripening phase, several enzymes are involved in starch hydrolysis, such as amylases, glucosidase, phosphorylase, sucrose synthase, and invertase.

During ripening changes in fat content occur. The effect of total acids and an increase in the degree of unsaturation of fatty acids. These changes occur only in the fraction of phospholipids. The total unsaturation remains practically constant during the pre-climateperiod. Linoleic and linolenic acids increase and then decrease during the climacteric period. All these changes are consistent with the hydrolysis and resynthesis of lipids during the ripening process [30].

3.2. Hydration properties and color analyses of flours plantain

The color of plantain flour evolved from green to yellow during ripening days, which was reflected in the color parameters (Table 2), with statistically significant effects ($P < 0.05$). The lightness of the flour (L^*) decreased during the 5 days of ripening, and the values of the parameter a^* decreased, reflecting a less intense green color in the days of ripening. The color parameter b^* was always positive (yellow hues) and followed a similar trend as L^* . This decrease was associated with the appearance of brown spots, a

Table 1

Proximate analyses of plantain flour during maturity, expressed in g/100 g dry matter.

Maturity (Day)	Ph	TSS	Aw	Moisture (g/100 g)	Fat (g/100 g)	Protein (N \times 6.25) (g/100 g)	Ash (g/100 g)	Carbohydrate (g/100 g)
1	6.22 \pm 0.18 ^a	1.10 \pm 0.151 ^a	0.28 \pm 0.015 ^a	5.34 \pm 0.17 ^a	1.12 \pm 0.032 ^a	2.96 \pm 0.15 ^a	3.12 \pm 0.093 ^a	87.4 \pm 0.12 ^a
2	6.20 \pm 0.11 ^a	1.80 \pm 0.112 ^b	0.17 \pm 0.011 ^b	5.15 \pm 0.11 ^b	1.56 \pm 0.024 ^b	3.32 \pm 0.14 ^b	2.92 \pm 0.043 ^b	87.2 \pm 0.14 ^b
3	6.14 \pm 0.71 ^b	2.10 \pm 0.162 ^b	0.23 \pm 0.013 ^c	4.67 \pm 0.15 ^c	2.38 \pm 0.043 ^c	3.67 \pm 0.13 ^c	2.58 \pm 0.072 ^c	86.7 \pm 0.22 ^c
4	6.11 \pm 0.13 ^c	2.20 \pm 0.031 ^c	0.26 \pm 0.025 ^a	6.54 \pm 0.25 ^d	2.61 \pm 0.034 ^c	4.23 \pm 0.16 ^d	1.97 \pm 0.094 ^d	84.7 \pm 0.25 ^d
5	6.10 \pm 0.13 ^c	2.40 \pm 0.133 ^d	0.34 \pm 0.023 ^d	7.23 \pm 0.16 ^e	3.27 \pm 0.051 ^d	3.75 \pm 0.12 ^e	1.81 \pm 0.081 ^e	83.2 \pm 0.16 ^e

TSS: Total soluble solids.

Values are means \pm standard deviation (n = 3).

Means with the same letter in a column are not statistically different from each other ($p < 0.05$).

Table 2
Hydration properties and color analyses of flours plantain during maturity.

Maturity day	Hydration properties				Color			
	WHC (g/g)	WBC (g/g)	OAC (g/g)	SV (g/g)	CEm	L*	a*	b*
1	5.12 ± 0.14 ^a	2.21 ± 0.062 ^a	1.68 ± 0.061 ^a	13.1 ± 0.11 ^a	1.45 ± 0.21 ^a	80.1 ± 0.62 ^a	1.35 ± 0.17 ^a	16.2 ± 0.112 ^a
2	4.65 ± 0.16 ^b	1.81 ± 0.054 ^b	1.85 ± 0.081 ^b	13.6 ± 0.14 ^b	2.12 ± 0.22 ^b	76.5 ± 0.68 ^b	1.12 ± 0.12 ^b	16.4 ± 0.093 ^a
3	4.11 ± 0.16 ^c	1.34 ± 0.063 ^c	2.14 ± 0.092 ^c	14.1 ± 0.10 ^c	2.84 ± 0.19 ^c	72.2 ± 0.56 ^b	0.79 ± 0.17 ^c	16.7 ± 0.124 ^b
4	5.38 ± 0.15 ^d	1.98 ± 0.042 ^c	2.38 ± 0.074 ^d	14.6 ± 0.12 ^d	3.36 ± 0.18 ^d	68.3 ± 0.87 ^c	0.52 ± 0.15 ^d	17.1 ± 0.121 ^c
5	3.72 ± 0.11 ^e	1.63 ± 0.071 ^e	2.61 ± 0.093 ^e	15.1 ± 0.15 ^e	3.86 ± 0.20 ^e	65.3 ± 0.95 ^d	0.47 ± 0.16 ^d	17.4 ± 0.123 ^d

WHC: Water Holding Capacity, WBC: Water Binding Capacity, OAC: Oil Absorption Capacity, SV: swelling volume, CEm: Emulsifying Capacity. Values with different letters in the same column are significantly different ($P < 0.05$). (n = 3).

physiological phenomenon that occurs during fruit ripening [29]. This result could be related to enzymatic reactions specific to polyphenoloxidase activity [3].

Fig. 2a shows the water holding capacity (WHC) and Fig. 2b shows the water binding capacity (WBC). The hydration characteristics of plantain flour at different days of ripening (Table 2) showed a significant decrease ($P \leq 0.005$) in WHC and WBC. Green plantain flour depends on the physical conditions of starch granules, which together with dietary fiber, resistant starch, proteins, and amylose form a more expansive matrix that leads to higher water retention capacity. The changes observed in these characteristics during maturation are consistent with the existence of a climacteric peak on day four (Fig. 2). Consequently, the decrease in hydration characteristics can be attributed to the breakdown of starch and the release of sugars. It is possible that the sugar interacts with the starch chains or with water and limits the availability of water for hydration. A significant increase in EmC ($P < 0.05$) was observed during the ripening days (Table 2). The high emulsification capacity was associated with hydrophobic amino acids, which are more exposed at the oil-water interface [31]. The values obtained for the emulsifying of the capacity of plantain flour could be used as emulsifiers and stabilizers in the formulation and production of meat, sauces, and dairy products.

The contents of OAC and SV increased during the ripening days and correlated with the increase in fat content ($P < 0.05$), indicating an emulsifying role of fat. The increase in SV is important for the food industry which produces baked goods such as binders and

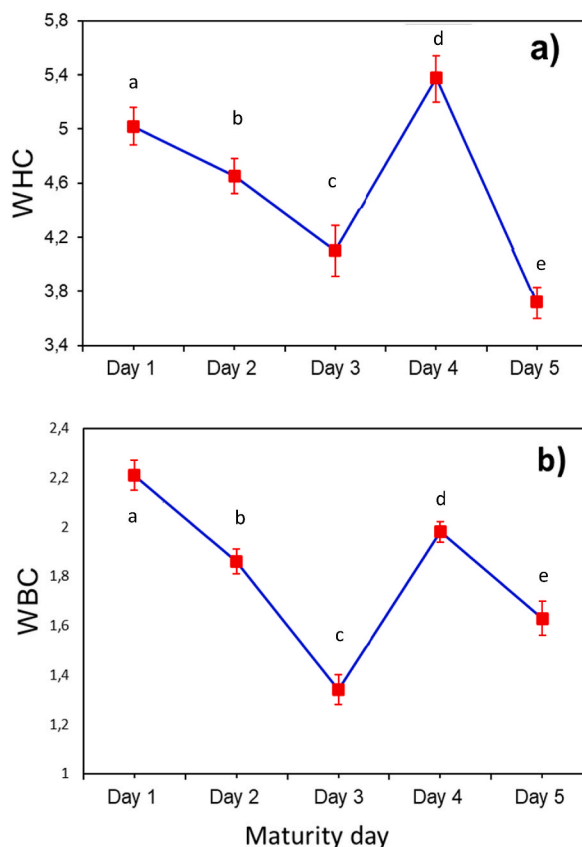


Fig. 2. a shows the WHC: Water Holding Capacity, b) WBC: Water Binding Capacity. The results are expressed as the mean ± SE of three independent experiments, in triplicates. Different letters express significant ($p < 0.05$).

thickeners.

Fig. 2a shows that WHC decreases with ripening and increases on the 4th day of ripening, indicating that it has the greatest ability to combine with water, a significantly different ($P < 0.05$). Polysaccharides such as dietary fiber and pectin in flour can bind and trap water molecules [32].

The WHC is mainly influenced by the degree of disintegration of the native starch granules as shown by the results of the analysis of SEM and can be attributed to dietary fiber, protein, and the physical state of the starch granules.

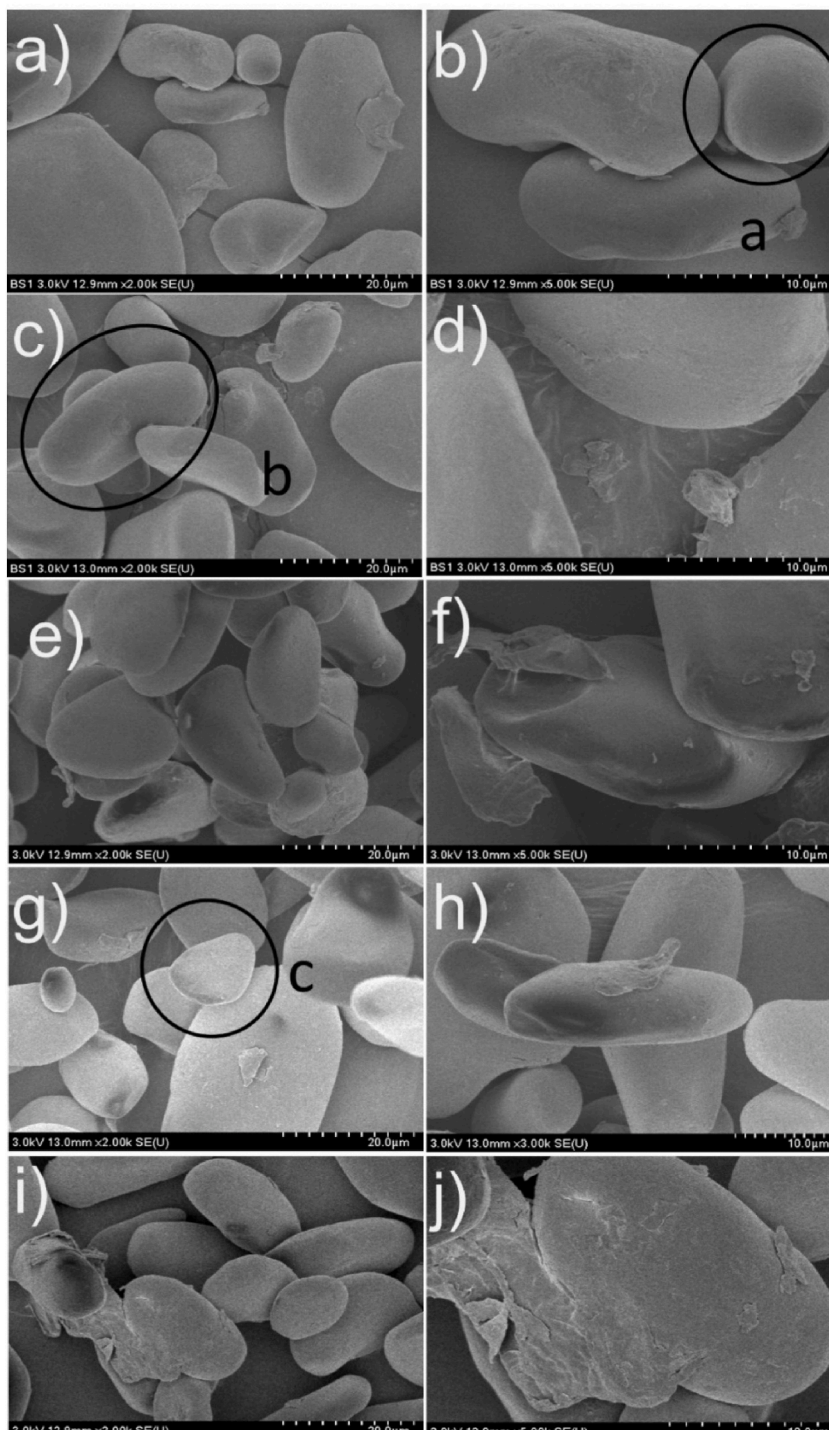


Fig. 3. a to j shows the SEM images of isolated starch along maturity from day 1 to day 5, taken at 2000 x and 5000x.

Water binding capacity (WBC) refers to the amount of water that the dry feed can absorb and is directly related to its hydration capacity. There was a significant difference ($p < 0.05$) between WBC during maturation days. The decrease in WBC could be due to protein denaturation. The water uptake of a protein is reduced by denaturation causing the hydrophobic groups migrate to the surface of the protein and reducing the amount of hydrogen bonding. Flours with high WBC are used as additives that cause rapid preparation of products because they can absorb large amounts of water even at low temperatures.

According to Ref. [33] the rapid change in swelling power (SV) at certain temperatures is due to the breakdown of intermolecular hydrogen bonding in the amorphous region, which allows gradual and irreversible water absorption. The nature of the arrangement of starch molecules (amylose and amylopectin), the size of the grains and their distribution also affect SV [34]. The results obtained for SV are related to their grain size, crystallinity and are important for the production and maintenance of the structure of various food such as bakery products, i.e., during and after the process.

3.3. Morphological changes in starch during maturity

Fig. 3a–j shows the SEM images of the isolated starches for different ripening stages, Fig. 2a and b for the first day, Fig. 3c and d for the second day, Fig. 3e and f for the third, Fig. 3g and h for the fourth, and Fig. 3i and j for the five days. Fig. 3 shows that the isolated starch has a lenticular (a), elliptical (b), and semispherical (c) shapes [1,34]. Lenticular has a diameter of 10–15 μm , for elliptical starches the length is between 15 and 32 μm and width between 10 and 15 μm , for semispherical starch the diameter ranges between 8 and 12 μm . As can be seen the metrology used to obtain isolated starch produce a clean sample with no fibers.

Most starch particles had a smooth surface during the first day of ripening while the surface of the starch particles became rough and wrinkled due to enzymatic effect as ripening progressed. The starches of plantain exhibited granules of different sizes with a smooth and dense surface, which can be related to resistance to enzymatic hydrolysis. The large granules are elongated, and the small granules are rounded. Smaller granules are probably those in process of formation, as the fruits are harvested at the green stage before starch degradation, which occurs during fruit ripening [34].

3.4. X-ray diffraction analysis

Fig. 4a shows the high-resolution X-ray diffraction (XRD) patterns of isolated plantain starches as a function of maturity. The origin

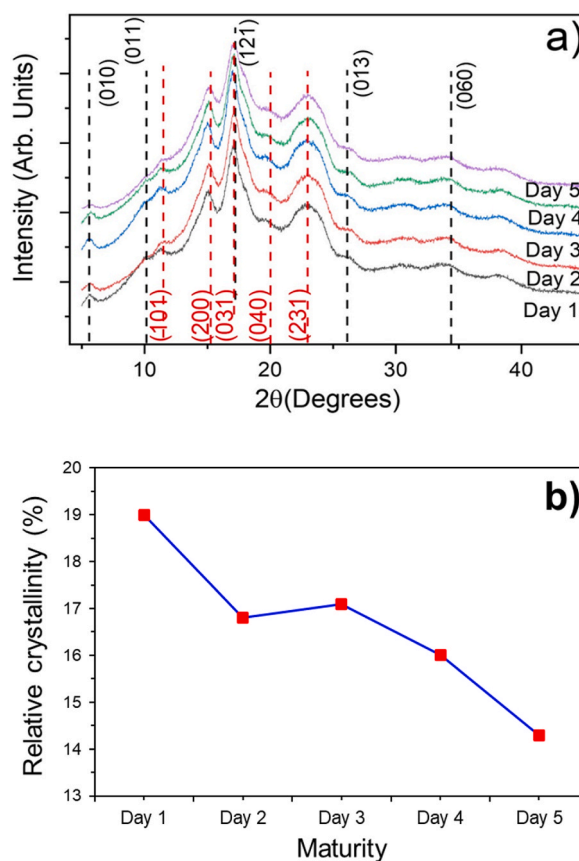


Fig. 4a. X-ray diffraction patterns of flour plantain during maturity, Fig. 4b changes in the apparent crystallinity as a function of the maturation.

of these patterns is due to the diffraction of the nanocrystals present in this starch. As was pointed out by Ref. [35], the presence of these nanocrystals produces the broadening of the diffracted peaks. From a crystallographic point of view these nanocrystals produce simultaneously elastic and inelastic X-ray scattering.

The black dashed lines correspond to indexing of the hexagonal structure, while red dashed lines correspond to orthorhombic crystalline structure, with the hexagonal phase predominating. This indexing was also reported by Ref. [1], for isolates Arton Dominic plantain starch. The orthorhombic structure is present in A-type starches such as amaranth and sorghum [36] and the hexagonal structure is present in B-type starches such as potato [37].

Here, it is important to recall that when both crystalline structures are in a starch, then, plantain starch is classified as C-type [15]. Plantain starch was classified as C-type, but they did not show X-ray pattern indexation.

Concerning the effect of the maturity on the crystalline structures of this isolated starch, if the maturity state increases there is a partial loss of the hexagonal and orthorhombic structures, reflecting a decrease of the relative crystallinity. The presence of both crystalline structures influences its thermal and pasting physicochemical properties.

The changes in the apparent crystallinity can be evaluated determining the crystalline region of the pattern. In the case of nanocrystals, the crystalline region of the pattern is formed by the elastic and inelastic scattering contributions. The calculation can be done, but if all the samples have the same inelastic contribution, it is possible to obtain the relative crystallinity [38].

Fig. 4b shows the changes in the relative crystallinity as a function of the maturation. This parameter was calculated by the determination of the crystalline area, the amorphous area, and the noise (electronic, instrumental, inelastic scattering by nanocrystals).

$$RC (\%) = \frac{\text{Crystalline area}}{\text{Total area} - \text{noise}} \quad (5)$$

As the maturity increases the relative crystallinity decreases, which means, that orthorhombic and hexagonal nanocrystals have been structurally modified. However, this is an open question that requires more work. Here is important to recall, that the existence of nanocrystals in starch during maturation has been not reported elsewhere.

3.5. Thermal properties

Fig. 5a shows the DSC thermograms for isolated starches as a function of maturity. The endothermic peak in this figure corresponds

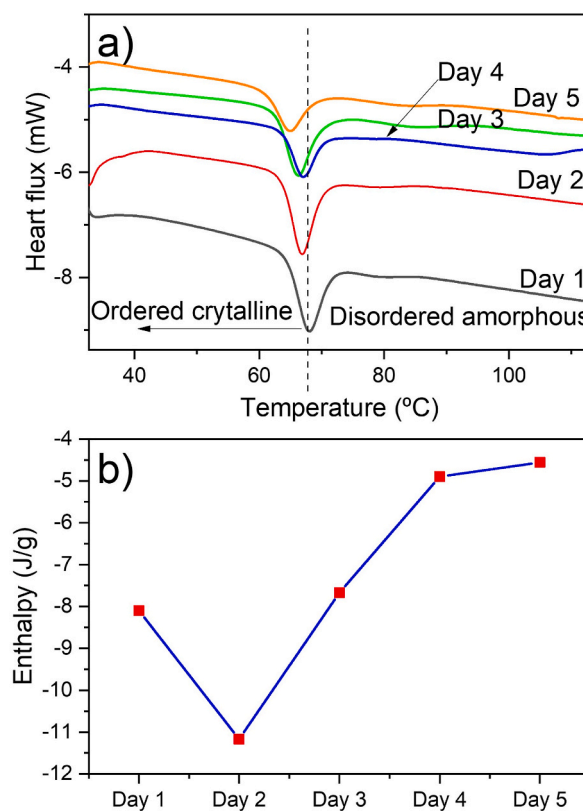


Fig. 5. a shows the DSC thermograms of plantain isolated starches as a function of the maturity, and Fig. 5b shows the changes in the enthalpy for the gelatinization.

to the gelatinization process. As shown in Fig. 4a Starch contains nanocrystals with orthorhombic and hexagonal structures that remains nearly integer at the earlier stages of maturity. From a vibrational point of view, the amplitude of the chemical bonds of these nanocrystals increases in the presence of water and heat from T_0 to T_p without changing their structures (ordered system). However, from T_p to T_e , the maximum amplitude of the bonds of the nanocrystals is broken and the system becomes disordered (amorphous), which means that gelatinization can be defined as a thermally irreversible transition in which the orthorhombic and hexagonal nanocrystals pass from an ordered system to a disordered system. As demonstrated by Ref. [39], the X-ray diffraction pattern of a sample before gelatinization shows an amorphous pattern.

Fig. 4b shows that as maturity increases, crystallinity decreases. Fig. 5b shows the changes in enthalpy (internal energy of the system) of these starches as a function of maturation. After the second day, there is a loss or gain of this parameter, which is directly related to the changes in crystallinity of the orthorhombic and hexagonal crystals according to Fig. 4a. The amylose/amylopectin complex occurs, but to a lesser extent than in other ripening stages, which is due to the early ripening reflected in the total solids ($^{\circ}$ Brix) (Table 1). In addition, the process of converting carbon to protein is reversed by the breakdown of starch, resulting in a decrease in the percent nitrogen from the first day of maturation. It is also important to mention that in this phase, some compounds, such as malate dehydrogenase, phosphorylase are present in oxidative processes, causing variations in the results.

In plantain starch, it is possible to identify the thermal transitions for orthorhombic and hexagonal nanocrystalline structures separately in DCS thermogram [1]. They showed for this isolated starch at the onset of ripening that both structures solvate, leading a double peak gelatinization, and that in the presence of water and heat, these nanocrystals undergo a solvation effect leading to the loss of their crystalline structure. A leftward shift can be seen in these thermograms with increasing maturity. For plantain starch, it can be confirmed from the X-ray and DSC measurements that the nanocrystals undergo small changes during ripening.

3.6. Pasting properties

Fig. 6a shows that the pasting profiles of plantain flours and Fig. 6 b shows the pasting profile of isolated plantain starches. As can be seen, flour profiles are altered by the degree of maturity, as reflected by the reduction in peak and final viscosity, but in the case of isolated starches, the peak viscosity increase and then decreases after day 3, this fact can be interpreted as a partial change in starch granules.

Pasting properties are related to intrinsic parameters such as grain size, grain integrity, amylose/amylopectin ratio, fat, protein and mineral content, and gelatinization of nanocrystals, among others. From Fig. 5a, T_g is about 68°C , and from Fig. 6a, gelatinization of orthorhombic and hexagonal nanocrystals does not affect the gelatinization profile in flours and starches. When the moisture content of starch is low, the gelatinization temperature is delayed. Extrinsic parameters such as moisture content, size of starch cumuli, and

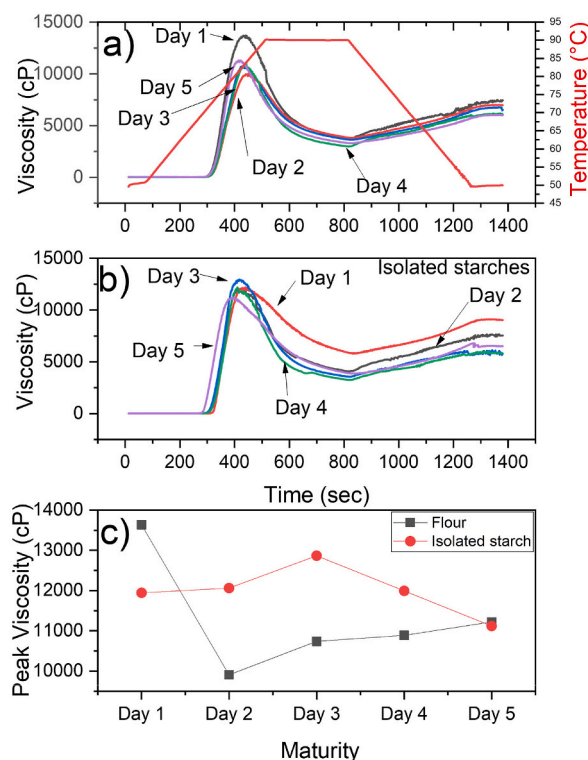


Fig. 6. a and b shows the pasting profiles of flour and isolated plantain starch for different degrees of maturity, Fig. 6c shows the changes in the peak viscosity as a function of the maturation day for flours and isolated starches.

changes in starch components due to modification processes also affect gelatinization. In this case, the pasting profiles correspond to isolated starches.

The evolution of the pasting profile using SEM images along pasting was studied by Ref. [39]. For starches rich in amylopectin, it was found that after the gelatinization temperature, the granules were completely disrupted, amylose and amylopectin were incorporated on the slurry, producing an increase in the apparent viscosity, no crystalline structures were found after gelatinization, and no starch retro gradation was reported. Recently, the changes in morphology along the paste profile in isolated avocado seed starch to understand the paste changes were studied [15]. In this case, a certain fraction of starch grains remains intact after gelatinization, as X-ray diffraction patterns for different points of a block paste still show the presence of structures in certain degree of crystallinity. This means that heat and water do not alter certain areas of the starch during gelatinization. In this case, these samples exhibit both hexagonal and orthorhombic nanocrystals. The paste profile behaves differently depending on the intrinsic properties of the starch grain studied. Fig. 6c shows changes in the peak viscosity for isolated starches and flours as a function of maturity. Slurries of flour and isolated starch behave between a custard and a hydrogel. According to Ref. [40], the slurry behaves like a custard when the end viscosity increases, but like a hydrogel when the end viscosity is lower than the peak viscosity.

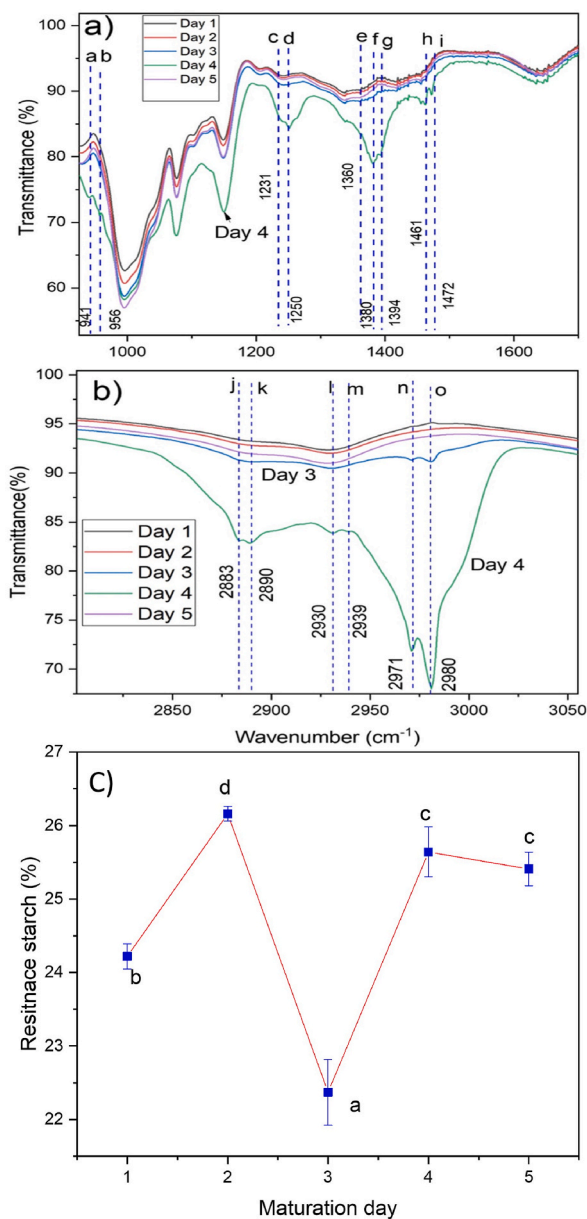


Fig. 7. a and b shows Infrared spectra of flour plantain during maturity: ν -stretching, δ -deformation, s -symmetrical, as -asymmetrical, st -strong, m -medium, and c) Changes in the resistant starch (RS) as a function of the maturity.

On the other hand, the decrease in the peak viscosity of plantain flour could be associated with the reduction on the fat content (Table 1); and in the case of isolated starches this parameter does not influence the changes in peak viscosity. These results indicate that both plantain flours and starches at different stages of maturation could be used as a functional ingredient for, prepare beverage or baby food due to the content of bioactive compounds as well as, its sugar and fat content that improve taste and palatability. Is an excellent gluten-free flour with low processing cost and can be used as a favorable substitute for wheat flour to improve the nutritional and functional characteristics of gluten-free products without affecting the overall acceptability of the products [41]. With the purpose to reach proper industrialization and health benefit for consumers, plantain flour has broad prospects for development and application as formulations in a variety of foods, such as pasta [42], dairy products [43], and bakery products baked goods. As a gluten-free flour rich in indigestible carbohydrates and antioxidants, the addition of plantain flour in functional foods is beneficial to improving the nutritional and functional properties of products.

3.7. Vibrational analysis

Fig. 7 a and b shows the IR spectra of flour plantain during maturity, letters were used to identify each one of the vibrational modes for each one of the starch components (fat, protein, amylose, amylopectin, orthorhombic and hexagonal nanocrystals). However, in the literature related to the assignation of the IR bands, there is a controversy about the identification of each vibrational state. The FTIR spectrum provides information on the chemical groups and their vibratory state that is related to the changes produced in the chemical composition of the plantain starch with different days of maturity to obtain starch. Two regions of interest were analyzed.

The band at 941 cm^{-1} (a) is due to C–C stretch vibrations exhibits small changes due to maturation; the band at 958 cm^{-1} (b) could be due to the degree of substitution during maturity; band at 1231 cm^{-1} (c) can be assigned to the $\nu\text{C-N}$ vibration; a strong absorption band at 1250 cm^{-1} (d) characterizes O-acetyl samples; band at 1360 cm^{-1} (e) is assigned to methyl asymmetric bending vibration; band at 1380 cm^{-1} (f) is characteristic of the angular deformation of the C–H bonds in starch; the band at 1394 cm^{-1} (g) corresponds to the symmetric stretching of carboxylate groups (–COO–); band at 1456 cm^{-1} (h) is assigned to C–H deformation vibration; the band at 1472 cm^{-1} (i) corresponds to the $\delta(\text{C-H})$ or $\delta(\text{CH}_2)$ in plane.

Fig. 7b shows the IR region in which there was more changes due to the maturation process, the band at 2882 cm^{-1} (j) corresponds to $\nu\text{st}(\text{C-H})$ or $\nu(\text{C-H})$ in CH_2/CH_3 group, and band at 2890 cm^{-1} (k) to $\nu\text{st}(\text{C-H})$ or $\nu(\text{C-H})$ in CH_2/CH_3 group, 2930 cm^{-1} (l) to $\nu(\text{C-H})$. The band at 2939 cm^{-1} (m) is due to the stretching vibration of the $-\text{CH}_2$ bonds, 2971 cm^{-1} (n) is due to $\nu(\text{C-H})$, $\nu(\text{-OH})$, 2980 cm^{-1} (o) with absorber water.

The flour of plantain has a similar composition and consists mainly of soluble fiber, soluble proteins, and fats. But according to this information and the extraction process, it is affected by ripening, especially on the 4th day. These changes are attributed to the climacteric peak, which is due to maturation in an uncontrolled environment where there may be temperature differences and variations in respiration and ethylene production, which is also reflected in the energy expenditure resulting from the consumption of proteins, as reported by Ref. [3]; accordingly, the results obtained in the percentage of nitrogen and protein. Now, there is not information about the vibrational modes of the hexagonal and orthorhombic nanocrystals, and it is an open problem.

3.8. Resistant starch

The changes during ripening are reflected in the percentage of resistant starch in the ripening days. Fig. 7c show a percentage of 24% resistant starch (RS) on day 1, while day 2 shows a slight increase in resistant starch to 26%, but day 3 shows a decrease to 22%, while days 4 and 5 show an increase again to 25%. In general, plantain exhibit physiological changes due to modifications of the cell walls caused by the conversion of starch and organic acids into sugars and volatile compounds associated with flavor and aroma. These changes occur from plantain harvest, i.e., day 1. It has been previously described those plantains are rich in starch, mainly in the form of resistant starch, which corresponds to raw native starch and is hardly hydrolyzable [44]. This behavior can be attributed to the fact that the samples were taken during the first five days of storage, and it is possible that the fruits have not yet fully ripened.

However, the increase in the resistant starch content can associate to the simple sugars such as fructose and sucrose have been used in the maturation process of plantain, it is necessary to generate sufficient lipids and proteins, to continue the metabolism of the plantain, while unused sugars are metabolized again to generate reserve starch [45]. This is the reason of increase in resistant starch on day 4 and 5.

Therefore, plantain flour is very resistant to digestive enzymes, and it is difficult for the enzymes to pass through the pores on the surface of starch granules into their interior. Due to the compact surfaces of its starch granules (Fig. 3) and the stable, long-branched double helix structure of type B starch. For that reason, it is important for consumption and agro-industrial processing of bananas considering the ripening day.

The central point of this work is to relate the resistance strength to the starch components. Fig. 4b shows that the relative crystallinity and enthalpy of starch nanocrystals decreases with ripening, implying that some of the starch granules are not gelatinized or are only partially gelatinized and may still be integer or semi-integer. This fact could be an indication that part of the resistant starch consists of starch grains that still have orthorhombic and hexagonal nanocrystals. For that reason, it can infer that the resistant starch content is not only for the crystalline structure, because the nanocrystal starch is part of the total resistant starch content.

This result is very important for the industry as it opens a new window of application for the development of products based on plantain flour, to produce products that does not contribute with the obesity problem in developing countries. Because the resistant starch content is major in comparison with other foods commonly used in the food industry. It was reported values for resistant starch content of potatoes are between 3.5 and 3.8%, sorghum grain from 2 to 8% and maize starch from 2 to 4% of resistant starch [43,46].

4. Conclusions

Ripening is a kinematic process involving all the components of plantain. Minerals, fat, proteins, and starch are used at different stages of ripening. Significant differences were found in the hydration properties WHC, WBC, and EmC of plantain flour due to biochemical reactions and ethylene production that produce a climacteric peak in plantain on the fourth day of ripening. The results obtained for SV are related to the type, grain size, crystallinity, and food industry use at earlier stages of ripening. SEM images showed no changes in the morphology of the isolated starch. However, the crystalline structure of the orthorhombic and hexagonal crystalline structures is partially lost with maturity. This indicates that these structures exhibit some degree of solvation, which is confirmed by the decrease in enthalpy as a function of maturity. These results allow the classification of plantains according to their degree of ripeness and subsequent agro-industrial processing. These results indicate that both flour and starch plantains at different stages of ripeness can be used for the preparation of baby food, as they can be easily swallowed by young children and contain have amino acids and proteins that could be useful in human nutrition.

Author contribution statement

Olga L. Torres-Vargas, M. E. Rodríguez-García: Conceived and designed the experiments; Performed the experiments; Analyzed and interpreted data; Contributed reagents, materials, analysis tools or data; Wrote the paper.

Marcela Gaytan-Martínez, Fernanda Castro-Campos, Beatriz M. Millán-Malo: Performed the experiments; Analyzed and interpreted data.

Data availability statement

Data will be made available on request.

Declaration of competing interest

The authors declare that they have no known competing financial interests or personal relationships that could have appeared to influence the work reported in this paper.

Acknowledgements

This work was financially supported Laboratorio Nacional de Caracterización de Materiales at CFATA-UNAM, campus Juriquilla, Authors want to than M. en C. Manuel Flores for the SEM images and Alvaro Javier Gonzales (Universidad del Quindío) for the physicochemical analysis assistance. And el Laboratorio de Alimentos, Instituto Interdisciplinario de las Ciencias, Universidad del Quindío.

References

- [1] L.J. Vega-Rojas, S.M. Londoño-Restrepo, M.E. Rodríguez-García, Study of morphological, structural, thermal, and pasting properties of flour and isolated starch from unripe plantain (*Musa paradisiaca*), *Int. J. Biol. Macromol.* 183 (2021) 1723–1731, <https://doi.org/10.1016/j.ijbiomac.2021.05.144>.
- [2] V.D. Quintero-Castaño, F.J. Castellanos-Galeano, C.I. Álvarez-Barreto, J.C. Lucas Aguirre, L.A. Bello-Pérez, M.E. Rodríguez-García, Starch from two unripe plantains and esterified with octenyl succinic anhydride (OSA): partial characterization, *Food Chem.* 315 (2020), 126241, <https://doi.org/10.1016/j.foodchem.2020.126241>.
- [3] A. Campuzano, C.M. Rosell, F. Cornejo, Physicochemical and nutritional characteristics of banana flour during ripening, *Food Chem.* 256 (2018) 11–17, <https://doi.org/10.1016/j.foodchem.2018.02.113>.
- [4] H.N. Ayo-Omogie, I.A. Adeyemi, E.T. Otunola, Effect of ripening on some physicochemical properties of cooking banana (musa ABB cardaba) pulp and flour, *Int. J. Food Sci. Technol.* 45 (12) (2010) 2605–2611, <https://doi.org/10.1111/j.1365-2621.2010.02432.x>.
- [5] H.N. Ayo-Omogie, O.S. Jolayemi, C.E. Chinma, Fermentation and blanching as adaptable strategies to improve nutritional and functional properties of unripe Cardaba banana flour, *J. Agric. & Food Res.* 6 (2021), 100214, <https://doi.org/10.1016/j.jafr.2021.100214>.
- [6] P. Singham, I. Genitha, R. Kumar, Comparative study of ripe and unripe banana flour during storage, *J. Food Process. Technol.* 5 (2014) 384, <https://doi.org/10.4172/2157-7110.1000384>.
- [7] F.A.H. Sardá, F.N. de Lima, N.T. López, A.D.O. Santos, E.D.C. Tobaruela, E.T. Kato, E.W. Menezes, Identification of carbohydrate parameters in commercial unripe banana flour, *Food Res. Int.* 81 (2016) 203–209, <https://doi.org/10.1016/j.foodres.2015.11.016>.
- [8] E.W. Menezes, C.C. Tadini, T.B. Tribess, A. Zuleta, J. Binaghi, N. Pak, F.M. Lajolo, Chemical composition and nutritional value of unripe banana flour (*Musa acuminata*, var. Nanicão), *Plant Foods Hum. Nutr. (Dordr.)* 66 (2011) 231–237, <https://doi.org/10.1007/s11130-011-0238-0>.
- [9] P.A. Dobranowski, A. Stintzi, Resistant starch, microbiome, and precision modulation, *Gut Microb.* 13 (1) (2021), 1926842, <https://doi.org/10.1080/19490976.2021.1926842>.
- [10] F.U. Lei, J.C. Tian, C.L. Sun, L.I. Chun, RVA and farinograph properties study on blends of resistant starch and wheat starch, *Agric. Sci. China* 7 (2008) 812–822, [https://doi.org/10.1016/S1671-2927\(08\)60118-2](https://doi.org/10.1016/S1671-2927(08)60118-2).
- [11] F.P. Tan, E. Beltranena, E.R.T. Zijlstra, Resistant starch: implications of dietary inclusion on gut health and growth in pigs: a review, *J. Anim. Sci. Biotechnol.* 12 (1) (2021) 1–15, <https://doi.org/10.1186/s40104-021-00644-5>.
- [12] M. Włodarczyk, K. Śliżewska, Efficiency of resistant starch and dextrins as prebiotics: a review of the existing evidence and clinical trials, *Nutrients* 13 (11) (2021) 3808, <https://doi.org/10.3390/nu13113808>.
- [13] E. Agama-Acevedo, S.L. Rodríguez-Ambríz, F.J. García-Suárez, F. Gutierrez-Mérez, G. Pacheco-Vargas, L.A. Bello-Pérez, Starch isolation and partial characterization of commercial cooking and dessert banana cultivars growing in Mexico, *Starch Stärke* 66 (3–4) (2014) 337–344, <https://doi.org/10.1002/star.201300125>.
- [14] C.A. Soares, F.H.G. Peroni-Okita, M. Borba Cardoso, R. Shitakubo, F.M. Lajolo, B.R. Cordenunsi, Plantain and banana starches: granule structural characteristics explain the differences in their starch degradation patterns, *J. Agric. Food Chem.* 59 (2011) 6672–6681, <https://doi.org/10.1021/jf201590h>.

- [15] E.A. Esquivel-Fajardo, E.U. Martínez-Ascencio, M.E. Oseguera-Toledo, S.M. Londoño-Restrepo, M.E. Rodríguez-García, Influence of physicochemical changes of the avocado starch throughout its pasting profile: combined extraction, *Carbohydr. Polym.* 281 (2022), 119048, <https://doi.org/10.1016/j.carbpol.2021.119048>.
- [16] M.E. Rodríguez-García, M.A. Hernández-Landaverde, J.M. Delgado, C.F. Ramírez-Gutiérrez, M. Ramírez-Cardona, B. Millán-Malo, S.M. Londoño -Restrepo, Crystalline structures of the main components of starch, *Food Sci. (N. Y.)* 37 (2021) 107–111, <https://doi.org/10.1016/j.cofs.2020.10.002>.
- [17] A.A. Khoozani, A.E.D.A. Bekhit, J. Birch, Effects of different drying conditions on the starch content, thermal properties, and some of the physicochemical parameters of whole green banana flour, *Int. J. Biol. Macromol.* 130 (2019) 938–946, <https://doi.org/10.1016/j.ijbiomac.2019.03.010>.
- [18] A.A.C.C. Chemists, *Approved Methods of the AACC, The Association*, 2000.
- [19] Aoac, Official methods of analysis of AOAC International, in: Gaithersberg: AOAC International, eighteenth ed., 2005, [https://doi.org/10.1016/0924-2244\(95\)90022-5](https://doi.org/10.1016/0924-2244(95)90022-5).
- [20] G. Buonaiuto, D. Cavallini, L.M.E. Mammi, F. Ghiaccio, A. Palmonari, A. Formigoni, G. Visentin, The accuracy of NIRS in predicting chemical composition and fibre digestibility of hay-based total mixed rations, *Ital. J. Anim. Sci.* 20 (1) (2021) 1730–1739, <https://doi.org/10.1080/1828051X.2021.1990804>.
- [21] A.J. García-Salcedo, O.L. Torres-Vargas, A. del Real, B. Contreras-Jiménez, M.E. Rodríguez-García, Pasting, viscoelastic, and physicochemical properties of chia (*Salvia hispanica* L.) flour and mucilage, *Food Struct.* 16 (2018) 59–66, <https://doi.org/10.1016/j.foostr.2018.03.004>.
- [22] F. Cornejo, C.M. Rosell, Physicochemical properties of long rice grain varieties in relation to gluten free bread quality, *LWT—Food Sci. Technol.* 62 (2) (2015) 1203–1210, <https://doi.org/10.1016/j.lwt.2015.01.050>.
- [23] T.A.A. Nasrin, A. Noomhorm, A.K. Anal, Physico-chemical characterization of culled plantain pulp starch, peel starch, and flour, *Int. J. Food Prop.* 18 (1) (2015) 165–177, <https://doi.org/10.1080/10942912.2013.828747>.
- [24] J.E. Cervantes-Ramírez, A.H. Cabrera-Ramírez, E. Morales-Sánchez, M.E. Rodríguez-García, M. de la L Reyes-Vega, A.K. Ramírez-Jiménez, B.L. Contreras-Jiménez, M. Gaytán-Martínez, Amylose-lipid complex formation from extruded maize starch mixed with fatty acids, *Carbohydr. Polym.* 246 (2020), 116555, <https://doi.org/10.1016/j.carbpol.2020.116555>.
- [25] E. Gutiérrez-Cortez, E. Hernández-Becerra, S.M. Londoño-Restrepo, M.E. Rodríguez García, Physicochemical characterization of Amaranth starch insulated by mechanical separations, *Int. J. Biol. Macromol.* 177 (2021) 430–436, <https://doi.org/10.1016/j.ijbiomac.2021.02.138>.
- [26] D. Surya Prabha, J. Sathesh Kumar, Assessment of banana fruit maturity by image processing technique, *J. Food Sci. Technol.* 52 (3) (2015) 1316–1327, <https://doi.org/10.1007/s13197-013-1188-3>.
- [27] J.L. Barrera, G.S. Arrazola, D.G. Cayón, Caracterización fisicoquímica y fisiológica del proceso de maduración de plátano Hartón (musa AAB Simmonds) en dos sistemas de producción, *Acta Agron.* 59 (1) (2010) 20–29. ISSN 0120-2812.
- [28] S. Pragati, I. Genitha, K. Ravish, Comparative study of ripe and unripe banana flour during storage, *J. Food Process. Technol.* 5 (11) (2014) 1, <https://doi.org/10.4172/2157-7110.1000384>.
- [29] J.L. Moreno, T. Tran, B. Cantero-Tubilla, K. López-López, L.A. Becerra Lopez-Lavalle, D. Dufour, Physicochemical and physiological changes during the ripening of banana (musaceae) fruit grown in Colombia, *IJFST (Int. J. Food Sci. Technol.)* 56 (2021) 1171–1183, <https://doi.org/10.1111/ijfs.14851>.
- [30] F. Sun, H. Chen, D. Chen, H. Tan, Y. Huang, D. Cozzolino, Lipidomic changes in banana (*musa cavendish*) during ripening and comparison of extraction by folch and bligh-dyer methods, *J. Agric. Food Chem.* 68 (40) (2020) 11309–11316, <https://doi.org/10.1021/acs.jafc.0c04236>.
- [31] S.C. Ubbor, E.N.T. Akobundu, Quality characteristics of cookies from composite flours of watermelon seed, cassava and wheat, *Pakistan J. Nutr.* 8 (7) (2009) 1097–1102, <https://doi.org/10.3923/pjn.2009.1097.1102>.
- [32] J.D.S.O. de Almeida, C.O. Dias, N.D. Arriola, B.S. de Freitas, A. de Francisco, C.L. Petkowicz, R.D. Amboni, Feijoa (*Acca sellowiana*) peel flours: a source of dietary fibers and bioactive compounds, *Food Biosci.* 38 (2020), 100789, <https://doi.org/10.1016/j.fbio.2020.100789>.
- [33] L.A. Bello-Pérez, P.C. Flores-Silva, E. Agama-Acevedo, E. Tovar, Starch digestibility: past, present, and future, *J. Sci. Food Agric.* 100 (14) (2020) 5009–5016, <https://doi.org/10.1002/jsfa.8955>.
- [34] C. de Barros Mesquita, M. Leonel, C.M.L. Franco, S. Leonel, E.L. Garcia, T.P.R. Dos Santos, Characterization of banana starches obtained from cultivars grown in Brazil, *Int. J. Biol. Macromol.* 89 (2016) 632–639, <https://doi.org/10.1016/j.ijbiomac.2016.05.040>.
- [35] B. Gong, W. Liu, H.W. Tan, D. Yu, Z. Song, L.A. Lucia, Understanding shape and morphology of unusual tubular starch nanocrystals, *Carbohydr. Polym.* 151 (2016) 666–675, <https://doi.org/10.1016/j.carbpol.2016.06.010>.
- [36] C.C. Pinto, P.H. Campelo, S. Michielon de Souza, Rietveld-based quantitative phase analysis of B-type starch crystals subjected to ultrasound and hydrolysis processes, *J. Appl. Polym. Sci.* 137 (47) (2020), 49529, <https://doi.org/10.1002/app.49529>.
- [37] P. Pineda-Gómez, A. Rosales-Rivera, E. Gutiérrez-Cortez, M.E. Rodríguez-García, M. E. Comparative analysis of the water diffusion in the corn grains, with and without pericarp during thermo-alkaline treatment, *Food Bioprod. Process.* 119 (2020) 38–47, <https://doi.org/10.1016/j.fbp.2019.10.006>.
- [38] S.M. Londoño-Restrepo, R. Jeronimo-Cruz, B.M. Millán-Malo, E.M. Rivera-Muñoz, M.E. Rodríguez-García, Effect of the nano crystal size on the X-ray diffraction patterns of biogenic hydroxyapatite from human, bovine, and porcine bones, *Sci. Rep.* 9 (1) (2019) 1–12, <https://doi.org/10.1038/s41598-019-42269-9>.
- [39] N.- Rincón-Londoño, L.J. Vega-Rojas, M. Contreras-Padilla, A.A. Acosta-Osorio, B. Millan-Malo, M.E. Rodriguez-Garcia, Analysis of thermal pasting profile in corn starch rich in amylose and amylopectin: physicochemical transformations, part II, *Int. J. Biol. Macromol.* 91 (2016) 106–114.
- [40] M. Cornejo-Villegas, N. Rincón-Londoño, A. Del Real-López, M.E. Rodríguez-García, The effect of Ca²⁺ ions on the pasting, morphological, structural, vibrational, and mechanical properties of corn starch–water system, *J. Cereal. Sci.* 79 (2018) 74–182, <https://doi.org/10.1016/j.jcs.2017.10.003>.
- [41] M. Radúnz, T.M. Camargo, C.F.P. Nunes, E.D.S. Pereira, J.A. Ribeiro, H.C. Dos Santos Hackbart, F. Da Fonseca Barbosa, Gluten-free green banana flour muffins: chemical, physical, antioxidant, digestibility and sensory analysis, *J. Food Sci. Technol.* 58 (2021) 1295–1301, <https://doi.org/10.1007/s13197-020-04638-5>.
- [42] O. Patiño-Rodríguez, E. Agama-Acevedo, G. Pacheco-Vargas, J. Alvarez-Ramírez, L.A. Bello-Pérez, Physicochemical, microstructural and digestibility analysis of gluten-free spaghetti of whole unripe plantain flour, *Food Chem.* 298 (2019), 125085, <https://doi.org/10.1016/j.foodchem.2019.125085>.
- [43] A.L.D. Batista, R. Silva, L.P. Cappato, M.V.S. Ferreira, K.O. Nascimento, A.G.G. Schmiele, Developing a synbiotic fermented milk using probiotic bacteria and organic green banana flour, *J. Funct. Foods* 38 (2017) 242–250, <https://doi.org/10.1016/j.jff.2017.09.037>.
- [44] R.A. Gonzalez-Soto, R. Mora-Escobedo, H. Hernandez-Sanchez, M. Sanchez-Rivera, L.A. Bello-Perez, The influence of time and storage temperature on resistant starch formation from autoclaved debranched banana starch, *Food Res. Int.* 40 (2) (2007) 304–310, <https://doi.org/10.1016/j.foodres.2006.04.001>.
- [45] N.A. Campos, S. Colombié, A. Moing, C. Cassan, D. Amah, R. Swennen, S.C. Carpentier, From fruit growth to ripening in plantain: a careful balance between carbohydrate synthesis and breakdown, *J. Exp. Bot.* 73 (14) (2022) 4832–4849, <https://doi.org/10.1093/jxb/erac187>.
- [46] S.K. Raatz, L. Idso, L.K. Johnson, M.I. Jackson, G.F. Combs Jr., Resistant starch analysis of commonly consumed potatoes: content varies by cooking method and service temperature but not by variety, *Food Chem.* 208 (2016) 297–300, <https://doi.org/10.1016/j.foodchem.2016.03.120>.